

Utilizing Spent Batteries to Fabricate Ni/ZnO-MnO₂ Electrodes for Electrochemical Ammonia Oxidation

To cite this article: Jiachao Yao *et al* 2021 *J. Electrochem. Soc.* **168** 126505

View the [article online](#) for updates and enhancements.



 The Electrochemical Society
Advancing solid state & electrochemical science & technology

243rd ECS Meeting with SOFC-XVIII

More than 50 symposia are available!



Present your research and accelerate science

Boston, MA • May 28 – June 2, 2023

[Learn more and submit!](#)



Utilizing Spent Batteries to Fabricate Ni/ZnO-MnO₂ Electrodes for Electrochemical Ammonia Oxidation

Jiachao Yao,¹ Yu Mei,¹  Zeyu Wang,² Jun Chen,^{1,2}  Dzmitry Hrynsphan,³ and Tatsiana Savitskaya³

¹College of Biology and Environmental Engineering, Zhejiang Shuren University, 310015 Hangzhou, People's Republic of China

²Interdisciplinary Research Academy, Zhejiang Shuren University, Hangzhou 310015, People's Republic of China

³Research Institute of Physical and Chemical Problems, Belarusian State University, 220030, Minsk, Belarus

In this work, a novel Ni/ZnO-MnO₂ electrode was fabricated by utilizing spent zinc-manganese batteries and then was applied to the electrochemical treatment of ammonia-containing wastewater. The obtained Ni/ZnO-MnO₂ electrode was characterized by scanning electron microscopy, X-ray diffraction, and linear scanning voltammetry, suggesting that the fabricated electrode had a flower-like structure and showed high oxygen evolution potential and electrochemical activity. The electrochemical performance of the ZnO-MnO₂ electrode in regard to ammonia removal and product selectivity was then investigated with different operating factors (i.e., electrolyte concentration, initial pH value, current density, and Cl⁻ concentration), and the results indicated that the ammonia removal efficiency could reach 100% with a N₂ selectivity of 91.8% under optimal conditions. Additionally, the mechanism of ammonia oxidation was proposed by cyclic voltammetry tests and active radical measurements, showing that ammonia was mainly oxidized via direct electron transfer, hydroxyl radicals, and active chlorine. Finally, the ZnO-MnO₂ electrode was equipped for the treatment of actual pharmaceutical wastewater, results for which showed that ammonia could be completely removed with a current efficiency of 26.2% and an energy consumption of 52.7 kWh/kg N. Thus, the ZnO-MnO₂ electrode prepared by recycling spent batteries is a promising anode for wastewater treatment.

© 2021 The Electrochemical Society ("ECS"). Published on behalf of ECS by IOP Publishing Limited. [DOI: 10.1149/1945-7111/ac3abb]

Manuscript submitted August 6, 2021; revised manuscript received October 17, 2021. Published December 2, 2021.

Incompletely treated wastewater discharge from human activities, including the pharmaceutical, landfill, and dyeing industries, usually contains a large amount of ammonia, which poses great threats to aquatic ecosystems and public health.^{1,2} Anammox process is presently the most appealing biological technology for the treatment of ammonia-containing wastewater;^{3,4} however, it highly relies on carbon resources, temperature, hydraulic retention time and pH.^{5,6} Other technologies for ammonia removal, such as photocatalysis,⁷ breakpoint chlorination,⁸ Fenton,⁹ and adsorption,¹⁰ have several drawbacks and may not achieve the required removal efficiencies while complying with increasingly stringent environmental regulations.¹¹

Electrochemical oxidation has attracted considerable attention and has emerged as a promising approach for wastewater treatment due to its environmental compatibility, versatility, and high efficiency, while producing no sludge.^{12–14} It is well known that anode materials play a crucial role in implementing electrochemical oxidation methods for pollutant degradation.^{15,16} Ideal electrode materials are usually inexpensive and exhibit high catalytic performance, a long service life, and environmental friendliness.^{17,18} Several typical electrodes have been reported as comparatively desirable anode materials. Boron-doped diamond (BDD) electrodes are considered one of the most efficient anodes because of their high oxygen evolution potential (OEP) and excellent electrochemical stability,¹⁹ however, their difficult preparation and high cost hinder their wide application.^{20,21} Lead dioxide (PbO₂) electrodes have been regarded as an excellent metal oxide electrode in view of their good corrosion resistance, high conductivity, and low cost;²² however, toxic Pb²⁺ may dissolve into the water.²³ In addition, Sb-doped SnO₂ (Sb-SnO₂) electrodes have garnered significant attention and have proven to be an outstanding electrode for ·OH production owing to their high OEP, unique crystalline structure and easy preparation,²⁴ but increasing their service life remains to be further investigated.²⁵ Compared with the above electrodes, MnO₂ electrodes have become one of the most promising alternatives due to their low toxicity, large surface area, and high catalytic activity.²⁶ For example, Orimolade et al.²⁷ prepared a modified MnO₂ film through pulsed layer deposition and observed enhanced

electrocatalytic degradation of emerging pharmaceutical pollutants. Shih et al.²⁸ developed a manganese dioxide electrode incorporating active carbon that could provide reactive sites for the electrosorption and electrocatalysis of contaminants; after optimization, the pollutant removal efficiency could reach 95%. Du et al.²⁹ summarized that, compared with other electrodes, manganese oxide electrodes, especially those with nanostructures, could provide specific polymorphisms to mediate electron transfer between the electrode and pollutant, thus enhancing the electrochemical performance for wastewater treatment.

Currently, the recycling of solid waste to maximize resource utilization and its elimination has attracted considerable attention. Zn-MnO₂ batteries are one of the most common solid wastes in human daily life, and these are mainly comprised of 12%–28% (w/w) Zn and 26%–45% (w/w) Mn.³⁰ If spent Zn-MnO₂ batteries are discarded optionally, they will inevitably cause soil and water pollution. As reported by Chen et al.,³¹ in addition to environmental problems, spent batteries can also pose human health risks, such as blood poisoning, hepatotoxicity, and nervous system diseases. In addition, Sun et al.³² presented that approximately 46%–75% of energy could be saved by recycling and using the metal from spent batteries rather than using only raw materials. Thus, improving the recycling of spent Zn-MnO₂ batteries and using the obtained materials as raw materials for reproduction will certainly alleviate their disposal problem and reduce their environmental impact. For instance, Ali et al.³³ proved the possibility of recycling spent batteries to fabricate MnO₂ supercapacitor electrodes, and the prepared electrode exhibited excellent electrochemical properties. It follows that it is possible to make use of Zn and Mn from spent Zn-MnO₂ batteries to prepare a novel electrode for electrochemical wastewater treatment.

In this work, a Ni/ZnO-MnO₂ anode was prepared using spent Zn-MnO₂ batteries and equipped for electrochemical treatment of ammonia-containing wastewater. The surface morphology, crystal structure, and electrochemical characteristics of the Ni/ZnO-MnO₂ electrode were studied. Then, the effects of electrolyte concentration, initial pH value, current density, and Cl⁻ concentration on the electrochemical performance of ammonia oxidation and product selectivity were investigated and optimized. Additionally, the mechanism of ammonia oxidation in the electro-oxidation system

was proposed. Finally, the Ni/ZnO-MnO₂ electrode was applied for the treatment of actual pharmaceutical wastewater to evaluate the possibility of industrialization.

Materials and Methods

Electrode preparation.—Spent Zn-MnO₂ batteries (Gold Peak Industry Group, China) were collected from a waste battery collection point in Hangzhou (China). Black paste was obtained by decomposing the spent batteries and separating the plastic films, paper pieces, and other dismantled products. The paste was dried for 24 h at 100 °C before being ground and sifted through a 75 μm sieve. The powder was ultrasonically cleaned several times with ultrapure water to remove the residual battery electrolyte. Subsequently, the washed powder was dried at 100 °C. Finally, the prepared powder was used to make a film on nickel foam to obtain the Ni/ZnO-MnO₂ anode (inspired by the work of Wang et al.³⁴). The Ni/ZnO and Ni/MnO₂ electrodes were prepared using the same method as commercial ZnO and MnO₂ powders (Macklin, China), respectively.

Electro-oxidation experiments.—Electro-oxidation experiments were conducted in a divided electrochemical cell separated by a proton exchange membrane (Nafion 117, DuPont) and equipped with the fabricated anode and a Ti cathode (both 2 cm × 2 cm). The inter-electrode gap was 3 cm. Additionally, 100 ml of simulated wastewater was stored in the anode chamber, and 100 ml of electrolyte with the same conductivity was loaded into the cathode chamber. The simulated wastewater was prepared by dissolving (NH₄)₂SO₄ in ultrapure water at an ammonia concentration of 50 mg N l⁻¹. Sodium sulfate was used as the supporting electrolyte. Chloride ions were supplied by adding sodium chloride. All electro-oxidation experiments were performed at 30 °C.

Analysis methods.—Ammonia and chemical oxygen demand (COD) were determined by Nessler reagent spectrophotometry and dichromate method, respectively.³⁵ Nitrate and nitrite were measured by ion chromatography.³⁶ N₂ was assayed by gas chromatography mass spectrometry.³⁶ The surface morphology was observed using a scanning electron microscopy (SEM, Hitachi, Japan). Moreover, X-ray diffraction pattern was obtained with an X-ray diffractometer (XRD, PANalytical, Netherlands). Hydroxyl radicals and active chlorine were measured by RNO and DPD standard methods, respectively.³⁷ Linear sweep voltammetry (LSV) and cyclic voltammetry (CV) were performed with an electrochemical workstation (CHI660E, Chenhua, China). The fabricated electrode was used as the working electrode, and a platinum sheet and a saturated calomel electrode (SCE) were used as the counter electrode and reference electrode respectively.

The N₂ selectivity was estimated as:³⁸

$$S_{N_2} = p \cdot \frac{C_{N_2}}{C_0 - C_t} \times 100\% \quad [1]$$

where p is the concentration of the targeted pollutant (mol) needed to form one mole of N₂, C_{N_2} is the produced N₂ concentration (mg L⁻¹), and C_0 and C_t are the ammonia concentrations at times 0 and t , respectively.

The current efficiency CE (%) for ammonia removal was calculated as follows:³⁹

$$CE = \frac{(C_0 - C_t)S_{N_2}}{14It} nFV \times 100\% \quad [2]$$

where I is the current supplied, F is the Faraday constant (96 485 C mol⁻¹), 14 is the atomic mass of N, and n is the electron transfer number from ammonia to N₂.

The energy consumption for the degradation of 1 kg of ammonia-N was estimated as follows:⁴⁰

$$E = \frac{UIt}{V \times (C_0 - C_t)} \quad [3]$$

where U is the voltage.

Results and discussion

Electrode characteristics.—Figure 1a shows the SEM images of the ZnO-MnO₂ coating of the Ni/ZnO-MnO₂ electrode. It was clearly observed that the surface of the electrode presented a flower-like structure with a mean diameter approximately 500 nm. The high surface roughness of the flower-like structure was expected to be conducive to enhancing the adhesion between the substrate and coating, and prolonging the service lifetime of the electrode.⁴¹ In addition, the large surface area could provide a better chance for electron movement, which would facilitate electron transfer between the electrode and pollutant.⁴² The XRD pattern was used to identify the phase structure of the fabricated electrode. As shown in Fig. 1b, four characteristic diffraction peaks at 2θ values of 21.034°, 37.120°, 42.401°, and 56.027° corresponded to the (001), (100), (101), and (102) crystal planes of MnO₂ (JCPDS 30-0820). The diffraction peaks at 2θ angles of 31.769°, 34.421°, 36.252°, 47.538°, 56.602°, 62.865° and 66.378° corresponded to the reflections of the (100), (002), (101), (102), (110), (103), and (200) crystal planes, thereby matching ZnO (JCPDS 36-1451).

To explore the electro-oxidation capability of the electrode, linear sweep voltammetry was performed to examine the oxygen evolution potential (OEP). Figure 2a shows the steady-state polarization curves on Ni/ZnO-MnO₂, Ni, commercial Ni/ZnO and Ni/MnO₂ electrodes. Among these electrodes, the OEP of the Ni/ZnO-MnO₂

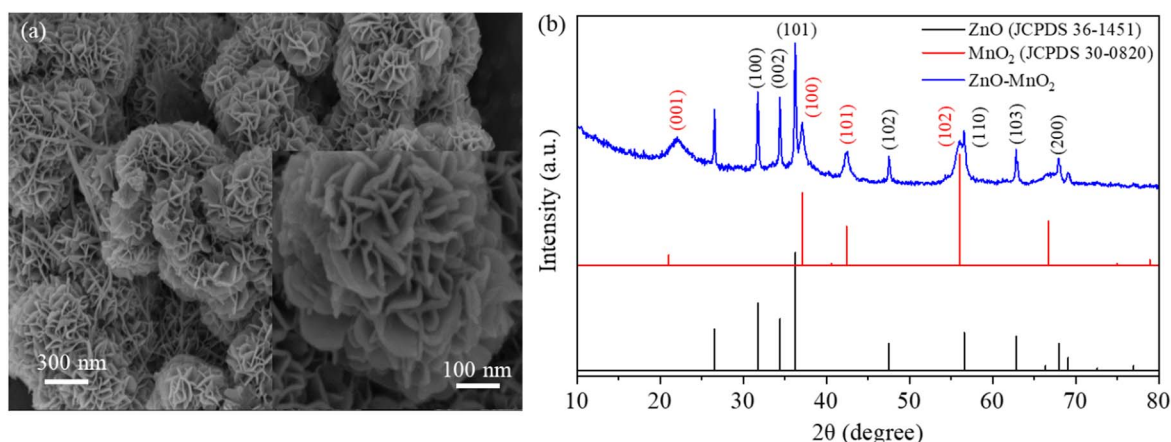


Figure 1. Characteristics of the prepared ZnO-MnO₂ electrode. (a) SEM image; (b) XRD pattern.

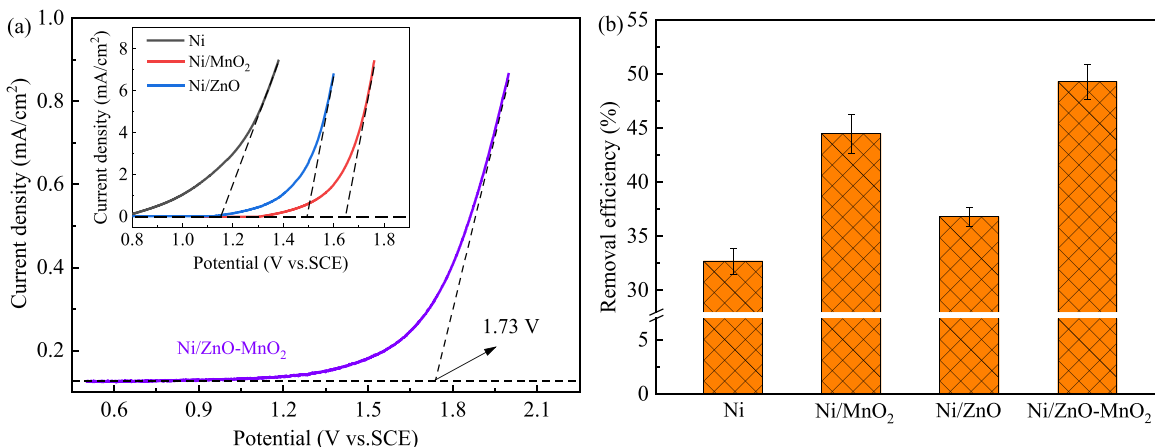


Figure 2. The comparison of electrochemical behaviors of the different electrodes. (a) steady-state polarization curves (0.5 mol/L H_2SO_4 , 100 mV s^{-1}); (b) ammonia removal performance (Electrolyte concentration of 0.1 mol L^{-1} , initial pH value of 6, current density of 10 mA cm^{-2} , no Cl^- , electrolysis time of 60 min).

electrode was found to be 1.73 V (vs. SCE), which was higher than those of Ni (1.16 V), Ni/ZnO (1.49 V) and Ni/MnO₂ (1.65 V). Such results indicated that the Ni/ZnO-MnO₂ electrode had the optimum performance for promoting pollutant oxidation and restraining the side reaction of oxygen evolution. Moreover, the ammonia removal efficiencies of the different electrodes were compared to further determine the electrochemical performance. As shown in Fig. 2b, the catalytic activity order of these four electrodes was Ni/ZnO-MnO₂ (49.3%) > Ni/MnO₂ (44.5%) > Ni/ZnO (36.8%) > Ni (32.7%), which was consistent with the relative OEP (Fig. 2a). These results were in agreement with conclusions reported elsewhere: there were unique active sites on the ZnO-MnO₂ interface that could effectively accelerate charge transfer and water splitting.^{43,44} According to the above results, it was considered that the Ni/ZnO-MnO₂ electrode had the potential for the electrochemical treatment of ammonia-containing wastewater.

Optimization of electrochemical ammonia oxidation.—To determine the electrochemical performance of the Ni/ZnO-MnO₂ electrode, the effects of electrolyte concentration, initial pH value, current density, and Cl^- concentration on ammonia removal and product selectivity were investigated.

The electrolyte concentration reflects the electroconductivity of the solution, which influences the electron transfer and pollutant degradation rate. Sodium sulfate was used as the supporting electrolyte, and concentrations varying from 0.05 mol L^{-1} to 0.3 mol L^{-1} were selected to study its effect on ammonia removal. As shown in Fig. 3a, the ammonia removal efficiency clearly increased at the beginning with increasing electrolyte concentration, i.e., reached a maximum value at 0.1 mol L^{-1} , and then gradually decreased as the electrolyte concentration was further increased. Such results might be related to the fact that the increase in electrolyte concentration could accelerate electron transfer; however, when the electrolyte concentration exceeded a certain value, excessive sulfate ions would be adsorbed on the electrode surface to form a salt layer, which could decrease the number of active sites on the electrode.⁴⁵ Figure 3b shows that N_2 was the main product during ammonia oxidation, while NO_3^- and NO_2^- were the byproducts. It also indicated that the electrolyte concentration had little effect on the product selectivity: N_2 selectivity was mainly stable in the range of 96% to 98%.

Solution pH value is one of the most important factors of electrochemical performance and can influence the existing form of pollutants and their intermediates.⁴⁶ Figure 4 shows the variation in ammonia removal and product selectivity as a function of the initial pH value. The results showed that an increase in the initial pH value had a positive effect on ammonia oxidation under acidic and

nonacidic conditions, respectively. Notably, alkaline conditions were more favorable for ammonia removal than other conditions. Nevertheless, the phenomenon of over-oxidation was easily occurred, i.e., the N_2 selectivity clearly decreased; the reason was related to the mechanism of direct electron transfer, which was reported in our previous work.⁴⁷ Considering the removal efficiency and N_2 selectivity, an initial pH value of 6.0 was selected.

Current density is a key factor that regulates the generation of active radicals during the electro-oxidation process. Figure 5a displays that there was an upward trend in ammonia removal as the current density was increased from 5 mA cm^{-2} to 20 mA cm^{-2} , and then a decreasing tendency was observed, suggesting that a maximum removal efficiency of 64.6% was obtained at 20 mA cm^{-2} . This explanation was connected with the oxygen evolution reaction (OER): an increase in current density was beneficial to produce active radicals to intensify the electrochemical performance; however, when the current density increased to a certain value, the excess energy was wasted on the OER, thus hindering pollutant removal.⁴⁸ Additionally, the N_2 selectivity decreased slightly from 97.7% to 94.9% with increasing current density, and then went stabilized.

Chloride ions are a common substance in actual wastewater. Thus, the effect of the Cl^- concentration on ammonia oxidation was studied, as shown in Fig. 6. When Cl^- was added to the solution, the ammonia removal efficiency sharply improved from 64.6% to 78.8% (500 mg l^{-1} Cl^-); and then ammonia was completely removed as Cl^- concentration reached 1000 mg l^{-1} . This finding was consistent with the results of other studies: the addition of Cl^- was favorable for generation of active chlorine, thus promoting the oxidation of ammonia.⁴⁰ In addition, the concentrations of generated chloramines were negligible during all experiments. Unfortunately, the reaction of ammonia over-oxidation was aggravated with increasing Cl^- concentration. The N_2 selectivity decreased from 94.9% (0 mg l^{-1} Cl^-) to 91.8% (1000 mg l^{-1} Cl^-) and then to 87.2% (1500 mg l^{-1} Cl^-). It was also found that NO_3^- was the main byproducts as Cl^- was added, indicating that NO_2^- was oxidized.

Mechanism of ammonia oxidation.—Cyclic voltammograms of the absence/presence of ammonia on the Ni/ZnO-MnO₂ electrode are presented in Fig. 7a. As shown, a pair of obvious redox peaks, i.e., an anodic current peak at ~1.04 V and a cathodic current peak at ~0.87 V, were observed in the presence of ammonia, indicating that direct electron transfer existed during ammonia oxidation.^{49,50} Figure 7b shows the cyclic voltammograms of ammonia oxidation as a function of the scan rate. When increasing the scan rate from 10 mV s^{-1} to 200 mV s^{-1} , the anodic current peaks moved slightly to more positive potentials; in other words, the ammonia oxidation

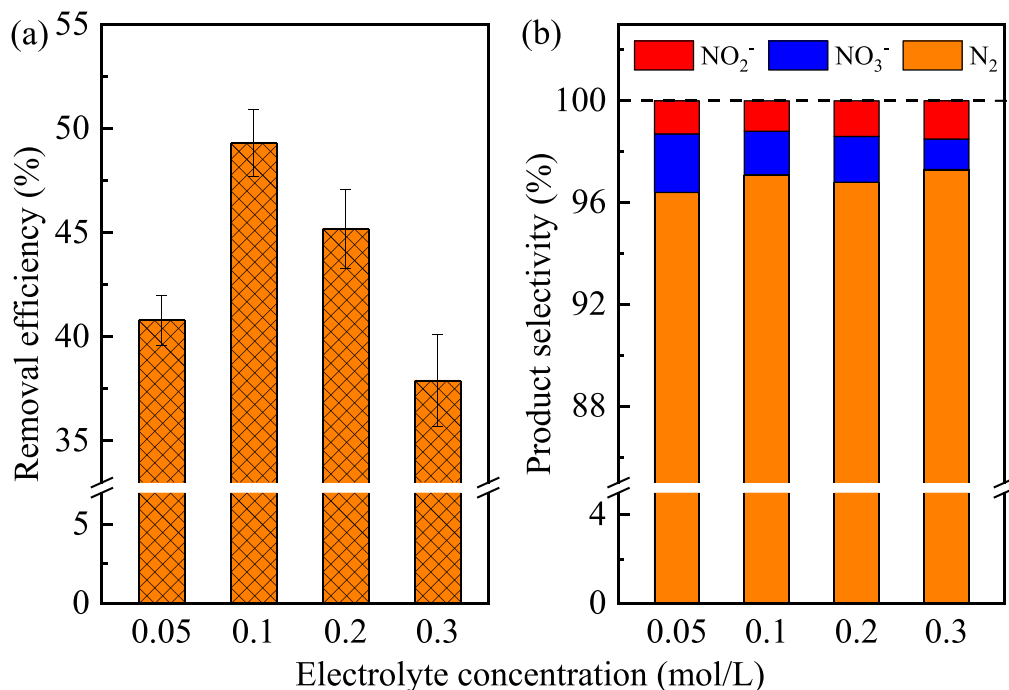


Figure 3. The effect of electrolyte concentration on ammonia removal. (Initial pH value of 6, current density of 10 mA cm^{-2} , no Cl^- , electrolysis time of 60 min)

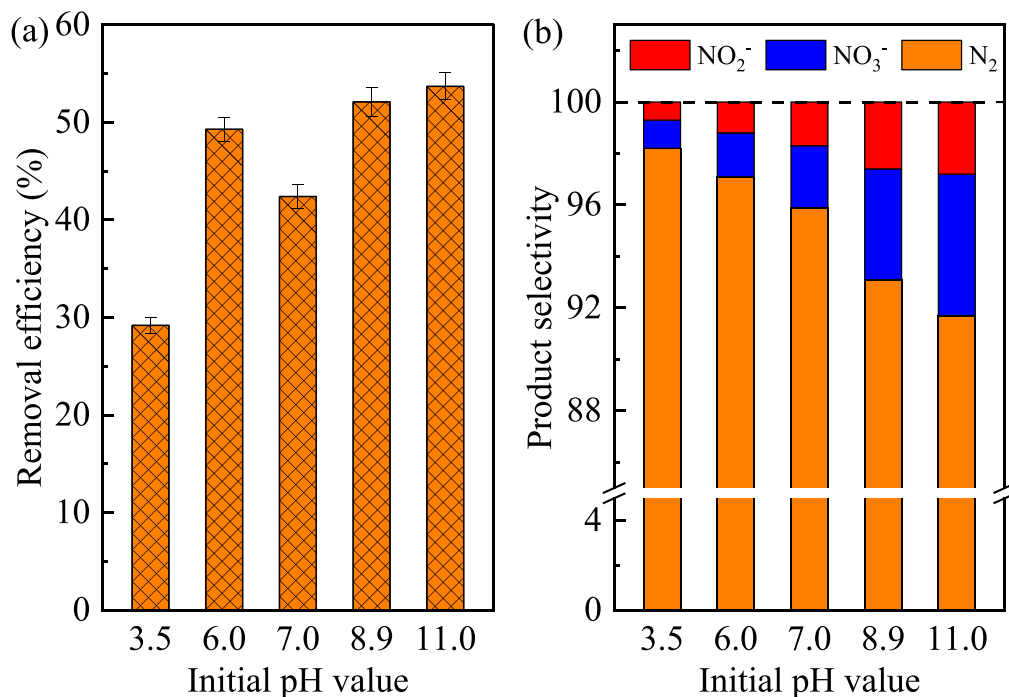


Figure 4. The effect of initial pH value on ammonia removal. (Electrolyte concentration of 0.1 mol L^{-1} , current density of 10 mA cm^{-2} , no Cl^- , electrolysis time of 60 min)

process was an irreversible process.⁵¹ The inset presented that there was a linear relationship between the anodic current peak and the square root of the scan rate, and the straight line did not pass the origin. This finding implied that diffusion-controlled theory was suitable for describing the ammonia oxidation process on the Ni/ZnO-MnO₂ electrode. Figure 7c displays that the generation of hydroxyl radicals and active chlorine increased with electrolysis, explaining that indirect oxidation greatly contributed to ammonia removal. Based on the above results, a schematic diagram of

mechanism of the electrochemical ammonia oxidation in anode chamber is shown in Fig. 7d, involving the ammonia oxidation mechanism by electrons, hydroxyl radicals and active chlorine. Most of the ammonia could be thoroughly transformed to N_2 , while some was converted to by-product such as nitrate and nitrite. Fortunately, the N_2 selectivity could consistently exceed 90% after optimization.

Verification of actual wastewater treatment.—For its possible practical application in the future, the oxidation performance of the

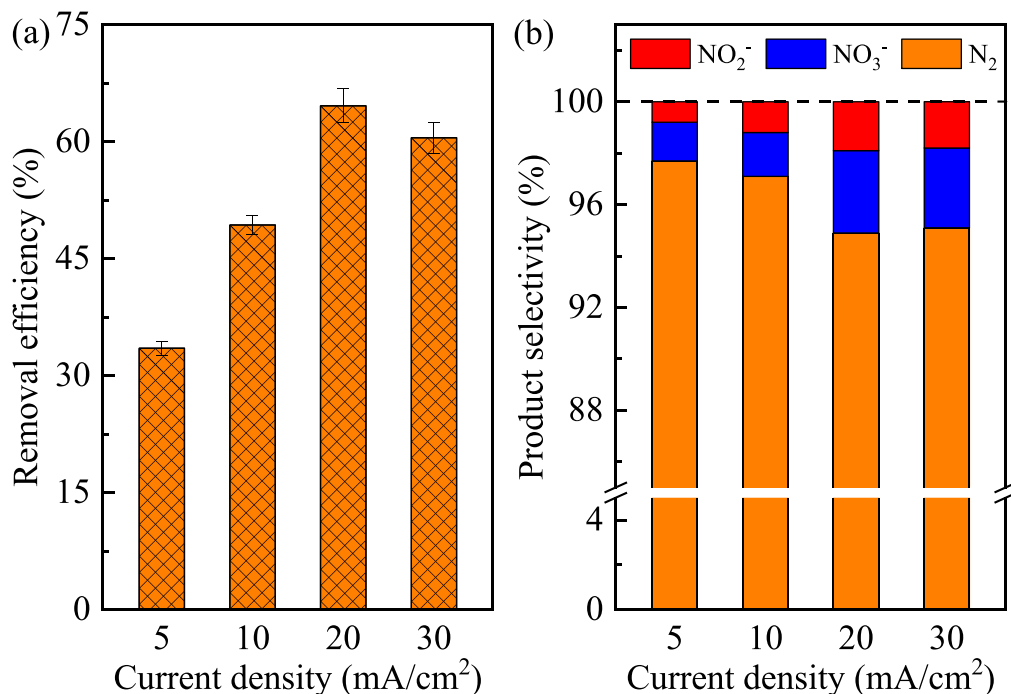


Figure 5. The effect of current density on ammonia removal. (Electrolyte concentration of 0.1 mol L⁻¹, initial pH value of 6.0, no Cl⁻, electrolysis time of 60 min)

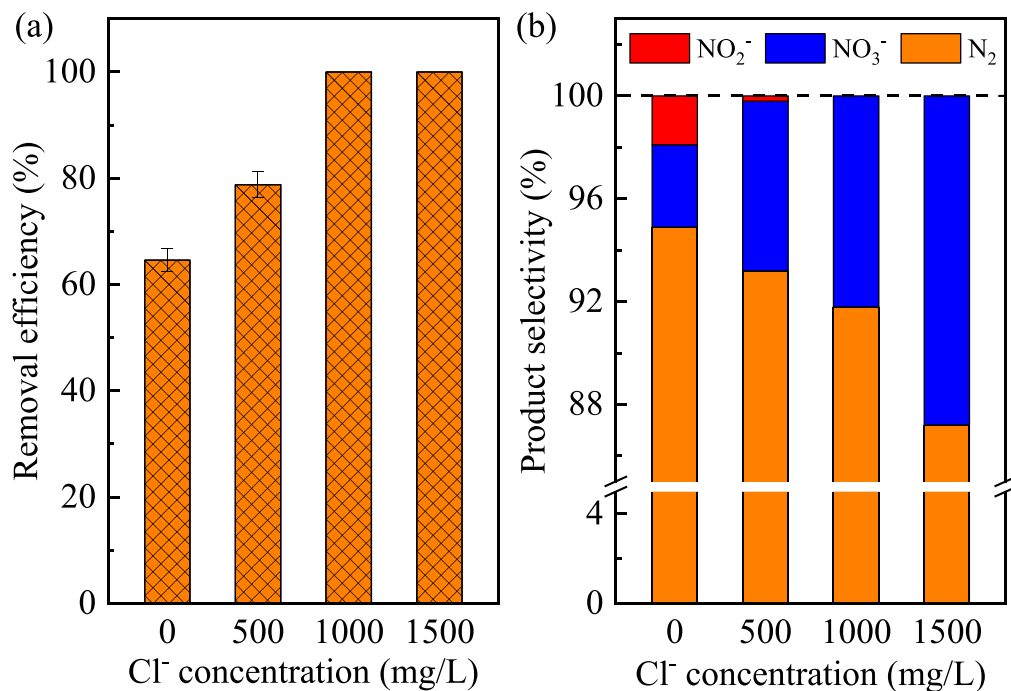


Figure 6. The effect of Cl⁻ concentration on ammonia removal. (Electrolyte concentration of 0.1 mol L⁻¹, initial pH value of 6.0, current density of 20 mA cm⁻², electrolysis time of 60 min)

fabricated electrode was tested in actual wastewater (i.e., effluent of secondary wastewater from a pharmaceutical factory, Zhejiang, China). Table I shows the characteristics of the actual wastewater and presents the results of electrochemical wastewater treatment. At a current density of 20 mA/cm² and an electrolysis time of 60 min, ammonia could be oxidized from 79 mg-N/L to 36 mg-N/L, and COD concentration decreased from 213 mg l⁻¹ to 128 mg/l. After another 60 min of electrolysis, ammonia was completely removed with a N₂ selectivity of 92.3%, and COD removal efficiency reached

73.2%. It was also observed that the effluent qualities after 120 min of electrolysis met the Discharge Standard of Water Pollutants for Pharmaceutical Industry in China. Besides, in order to evaluate the safety of the treated wastewater, the concentrations of the dissolved metal ions were measured by inductively coupled plasma mass spectrometry. The results indicated that the ion concentrations of manganese and zinc were 0.009 mg l⁻¹ and 0.006 mg l⁻¹, respectively, which met the Standard for Drinking Water Quality (manganese ≤ 0.1 mg l⁻¹; zinc ≤ 1.0 mg/l). Additionally, a current

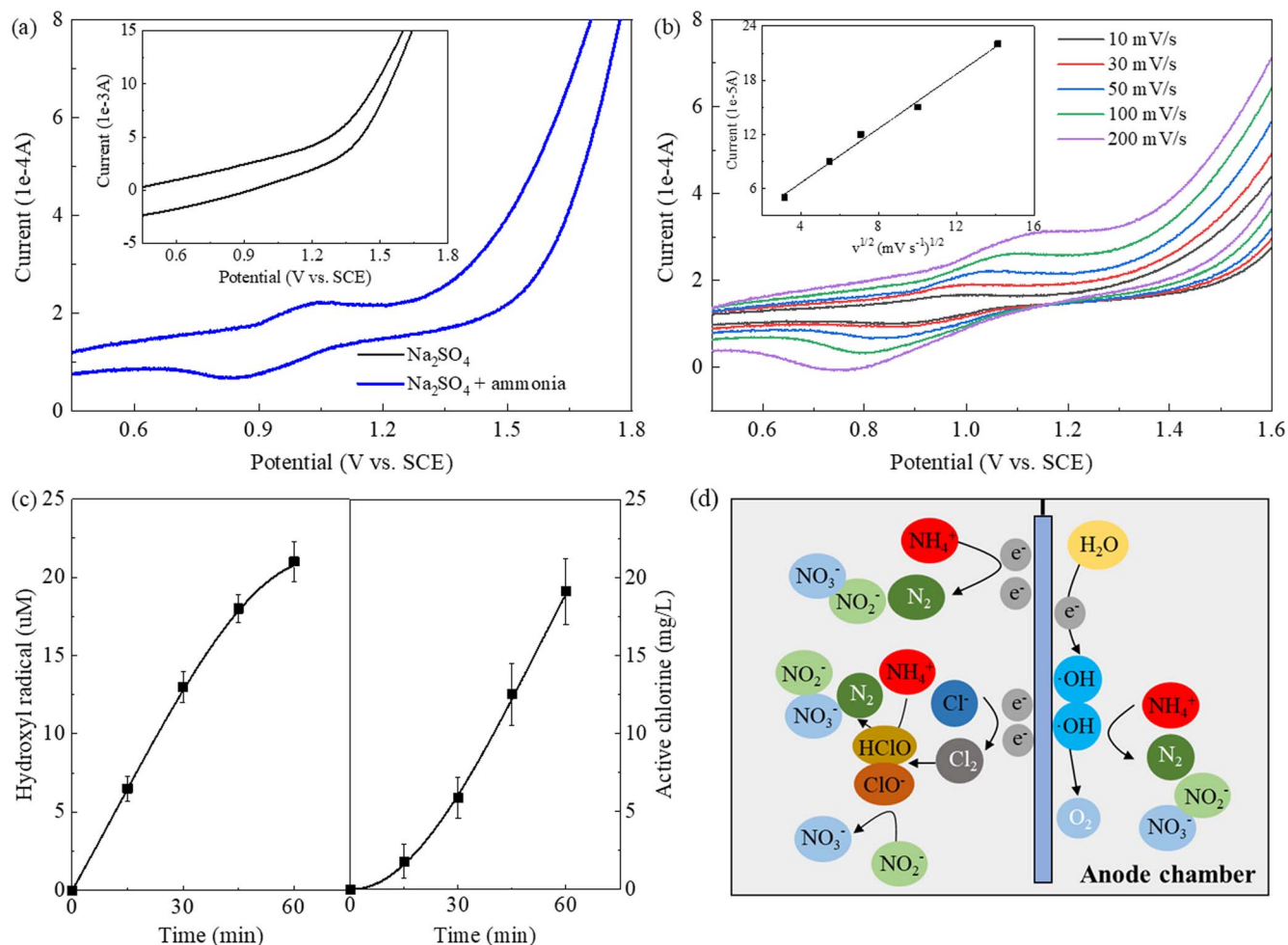


Figure 7. Mechanism for ammonia oxidation. (a) cyclic voltammograms of ammonia oxidation (electrolyte concentration of 0.1 mol L^{-1} , initial pH value of 6.0, no Cl^- , scan rate of 50 mV s^{-1}); (b) cyclic voltammograms with different scan rates (electrolyte concentration of 0.1 mol L^{-1} , initial pH value of 6.0, no Cl^-); (c) hydroxyl radical and active chlorine generation (electrolyte concentration of 0.1 mol L^{-1} , initial pH value of 6.0, current density of 20 mA cm^{-2} , 1000 mg/l Cl^-); (d) schematic diagram of mechanism of electrochemical ammonia oxidation in anode chamber.

Table I. The characteristics of actual wastewater before and after electrochemical treatment.

Parameter	Initial value	60 min treatment	120 min treatment	Discharge standard
Ammonia (mg-N/L)	79 ± 4	36 ± 4	ND	20
COD (mg/L)	213 ± 15	118 ± 13	57 ± 6	100
Color	15	ND	ND	50
pH	8.5 ± 0.2	7.6 ± 0.3	6.8 ± 0.2	6–9
Cl^- (mg/L)	876 ± 41	858 ± 38	849 ± 33	/

ND: not detected.

efficiency of 26.2% was obtained for ammonia removal, and energy consumption was calculated as 52.7 kWh/kg N . Compared with other electrode materials reported for ammonia-containing wastewater treatment (Table II), this Ni/ZnO-MnO_2 electrode was not only cost-effective in regard to its materials and operation but also exhibited excellent pollutant removal efficiency and energy saving during ammonia oxidation.

Conclusion

A Ni/ZnO-MnO_2 electrode was successfully prepared by recycling spent zinc-manganese batteries, and its electrochemical performance for the removal of ammonia from simulated and actual wastewater was evaluated in this study. The SEM, XRD, and LSV were applied to determine the electrode characteristics; results

showed that the flower-like structure electrode had an OEP of 1.73 V, which was more suitable for ammonia oxidation than that of other commercial electrodes. The operating parameters, including electrolyte concentration, initial pH value, current density, and Cl^- concentration, were investigated to reveal their effects on the ammonia removal and product selectivity by the Ni/ZnO-MnO_2 electrode. After optimization, 100% ammonia could be removed from the simulated wastewater, and N_2 was considered the main product. Then, the mechanism of direct and indirect electrochemical ammonia oxidation was presented via cyclic voltammetry and active radical tests. Additionally, the oxidation performance of the fabricated electrode was validated by treating actual pharmaceutical wastewater. The results indicated that the removal efficiencies of

Table II. Comparison of oxidation performance of different anode materials for ammonia removal.

Electrode material		Experimental conditions	Results			References
Anode	Cathode		Removal efficiency	Current efficiency	Energy consumption (kWh/kg N)	
graphite/PbO ₂	Graphite	100 mg/l NH ₄ ⁺ , 900 mg l ⁻¹ Cl ⁻ , current of 0.3 A, 120 min electrolysis	96.5%	~4.8%	/	52
Graphite/MnO	Graphite	1.42 mM NH ₄ ⁺ , 50 mM Cl ⁻ , current density of 3.5 mA cm ⁻² , 120 min electrolysis	~28%	17.8%	/	53
Ti/EBNTA	Ti/EBNTA	21 mM NH ₄ ⁺ , 30 mM Cl ⁻ , current density of 5 mA cm ⁻² , 240 min electrolysis	~75%	/	100	54
Ti/IrO ₂ -RuO ₂	Ti	50 mg/l NH ₄ ⁺ , 20 mM Cl ⁻ , pH 6.0, current density of 3 m A /c m ² , 40 min electrolysis	~95%	14.6%	126	55
Graphite	Stainless steel	185 mg/l NH ₄ ⁺ , 7500 mg L ⁻¹ Cl ⁻ , pH 8.93, current density of 40 m A /c m ² , 120 min electrolysis	~99%	~8%	491.9	56
Ti/Ir _{0.7} Ta _{0.3} O ₂ /Co-TiO ₂ /Sb-SnO ₂	Stainless steel	12 mM NH ₄ ⁺ , 60 mM Cl ⁻ , current density of 25 m A /c m ² , 120 min electrolysis	100%	/	383	57
Ni/ZnO-MnO ₂	Ti	79 mg/l NH ₄ ⁺ , 213 mg/l COD, pH 8.5, 876 mg l ⁻¹ Cl ⁻ , current density of 20 mA cm ⁻² , 120 min electrolysis	100%	26.2%	52.7	In this study

EBNTA: structurally enhanced blue-black TiO₂ nanotube array

ammonia and COD could reach 100% and 73.2%, respectively, and an energy consumption of 52.7 kWh/kg N was calculated.

Acknowledgments

The authors are grateful for the financial support provided by the National Primary Research & Development Plan (2018YFE0120300), National Natural Science Foundation of China (NO.22011530015), Natural Science Foundation of Zhejiang Province (NO.LGF20E020002), and Zhejiang Shuren University Basic Scientific Research Special Funds (NO.2022XZ006).

ORCID

Yu Mei  <https://orcid.org/0000-0002-2278-3865>

Jun Chen  <https://orcid.org/0000-0003-2695-4673>

References

- J. Y. Ye, J. L. Lin, Z. Y. Zhou, Y. H. Hong, T. Sheng, M. Rauf, and S. G. Sun, *J. Electroanal. Chem.*, **819**, 495 (2018).
- S. Chung, J. Chung, and C. Chung, *J. Water Process Eng.*, **37**, 101425 (2020).
- M. Landreau, S. J. Byson, H. You, D. A. Stahl, and M. K. H. Winkler, *Water Res.*, **183**, 116078 (2020).
- X. Yu, F. Nishimura, and T. Hidaka, *Bioresour. Technol.*, **317**, 123960 (2020).
- Y. Liu, H. H. Ngo, W. Guo, L. Peng, D. Wang, and B. Ni, *Environ. Int.*, **123**, 10 (2019).
- C. L. Madeira and J. C. de Araújo, *Sci. Total Environ.*, **799**, 149449 (2021).
- M. Bahmani, K. Dashtian, D. Mowla, F. Esmailzadeh, and M. Ghaedi, *J. Hazard. Mater.*, **393**, 122360 (2020).
- W. L. Wang, Q. Y. Wu, Y. Du, N. Huang, and H. Y. Hu, *Water Res.*, **129**, 115 (2018).
- L. Jurczyk and J. Koc-Jurczyk, *Waste Manag.*, **63**, 310 (2017).
- H. Cheng, Q. Zhu, and Z. Xing, *J. Clean. Prod.*, **233**, 720 (2019).
- A. A. Babaei, B. Kakavandi, M. Rafiee, F. Kalantarhormizi, I. Purkaram, E. Ahmadi, and S. Esmaeili, *J. Ind. Eng. Chem.*, **56**, 163 (2017).
- Y. J. Shih, Y. H. Huang, and C. P. Huang, *Electrochim. Acta*, **257**, 444 (2017).
- H. Zöllig, A. Remmele, E. Morgenroth, and K. M. Udert, *Environ. Sci.-Wat. Res.*, **3**, 480 (2017).
- N. Kaabi, B. Chouchene, W. Mabrouk, F. Matoussi, and E. S. B. H. Hmida, *Solid State Ionics*, **325**, 74 (2018).
- S. Johnston, B. H. R. Suryanto, and D. R. MacFarlane, *Electrochim. Acta*, **297**, 778 (2019).
- L. Labiadh, A. Barbucci, M. P. Carpanese, A. Gadri, S. Ammar, and M. Panizza, *J. Electroanal. Chem.*, **766**, 94 (2016).
- F. Almomani, R. Bhosale, M. Khraisheh, A. Kumar, and M. Tawalbeh, *Int. J. Hydrogen Energ.*, **45**, 10398 (2020).
- M. H. M. T. Assumpção, R. M. Piasentin, P. Hammer, R. F. B. De Souza, G. S. Buzzo, M. C. Santos, E. V. Spinacé, A. O. Neto, and J. C. M. Silva, *Appl. Catal. B: Environ.*, **174-175**, 136 (2015).
- V. Schmalz, T. Dittmar, D. Haaken, and E. Worch, *Water Res.*, **43**, 5260 (2009).
- J. B. Welter, S. W. da Silva, D. E. Schneider, M. A. S. Rodrigues, and J. Z. Ferreira, *Chemosphere*, **248**, 126062 (2020).
- K. E. Carter and J. Farrell, *Environ. Sci. Technol.*, **42**, 6111 (2008).
- J. M. Aquino, R. C. Rocha-Filho, L. A. M. Ruotolo, N. Bocchi, and S. R. Biaggio, *Chem. Eng. J.*, **251**, 138 (2014).
- J. Li, M. Li, D. Li, Q. Wen, and Z. Chen, *Chemosphere*, **248**, 126021 (2020).
- X. Li, Y. Wu, W. Zhu, F. Xue, Y. Qian, and C. Wang, *Electrochim. Acta*, **220**, 276 (2016).
- B. Wang, W. Kong, and H. Ma, *J. Hazard. Mater.*, **146**, 295 (2007).
- M. R. Majidi, F. Shahbazi Farahani, M. Hosseini, and I. Ahadzadeh, *Bioelectrochemistry*, **125**, 38 (2019).
- B. O. Oromolade, B. N. Zwane, B. A. Koiki, L. Tshwenya, G. M. Peleyeju, N. Mabuba, M. Zhou, and O. A. Arotiba, *J. Environ. Chem. Eng.*, **8**, 103607 (2020).
- Y. J. Shih, C. P. Huang, Y. H. Chan, and Y. H. Huang, *J. Hazard. Mater.*, **379**, 120759 (2019).
- X. Du, M. A. Oturan, M. Zhou, N. Belkessa, P. Su, J. Cai, C. Trelu, and E. Mousset, *Appl. Catal. B: Environ.*, **296**, 120332 (2021).
- V. S. Morais, R. V. Barrada, M. N. Moura, J. R. Almeida, T. F. M. Moreira, G. R. Gonçalves, S. A. D. Ferreira, M. F. F. Lelis, and M. B. J. G. Freitas, *J. Environ. Chem. Eng.*, **8**, 103716 (2020).
- F. Chen, M. Tan, J. Ma, S. Zhang, G. Li, and J. Qu, *J. Hazard. Mater.*, **302**, 250 (2016).
- M. Sun, X. Yang, D. Huisin, R. Wang, and Y. Wang, *J. Clean. Prod.*, **107**, 775 (2015).
- G. M. Ali, M. M. Yusoff, E. R. Shaaban, and K. F. Chong, *Ceram. Int.*, **43**, 8440 (2017).
- G. J. Wang, J. Gao, L. J. Fu, N. H. Zhao, Y. P. Wu, and T. Takamura, *J. Power Sources*, **174**, 1109 (2007).
- H. A. Hasan, S. R. S. Abdullah, S. K. Kamarudin, N. T. Kofli, and N. Anuar, *Sep. Purif. Technol.*, **130**, 56 (2014).
- J. Chen, S. Y. Gu, H. H. Hao, and J. M. Chen, *Appl. Microbiol. Biotechnol.*, **100**, 9787 (2016).
- J. Yao, A. Chen, R. Ye, J. Wang, H. Pan, D. Xu, J. Chen, Y. Mei, D. Hrynsphan, and T. Savitskaya, *J. Electrochem. Soc.*, **168**, 023502 (2021).
- J. Yao, Y. Mei, T. Yuan, J. Chen, H. Pan, and J. Wang, *J. Electroanal. Chem.*, **882**, 115019 (2021).
- J. Yao, B. Pan, R. Shen, T. Yuan, and J. Wang, *Sci. Total Environ.*, **687**, 198 (2019).
- J. Sun, L. Liu, and F. Yang, *Sci. Total Environ.*, **776**, 146035 (2021).
- X. Zhang, D. Shao, W. Lyu, G. Tan, and H. Ren, *Chem. Eng. J.*, **361**, 862 (2019).
- Y. Xia, Q. Dai, and J. Chen, *J. Electroanal. Chem.*, **744**, 117 (2015).
- M. W. Kim, B. Joshi, E. Samuel, H. Seok, A. Aldalbahi, M. Almoqli, M. T. Swihart, and S. S. Yoon, *Appl. Catal. B: Environ.*, **271**, 118928 (2020).
- M. Huang, F. Li, X. L. Zhao, D. Luo, X. Q. You, Y. X. Zhang, and G. Li, *Electrochim. Acta*, **152**, 172 (2015).
- Q. Dai, J. Zhou, M. Weng, X. Luo, D. Feng, and J. Chen, *Sep. Purif. Technol.*, **166**, 109 (2016).
- S. Singh, S.-L. Lo, V. C. Srivastava, Q. Qiao, and P. Sharma, *J. Taiwan Inst. Chem. E.*, **118**, 169 (2021).
- J. Yao, M. Zhou, D. Wen, Q. Xue, and J. Wang, *J. Electroanal. Chem.*, **776**, 53 (2016).
- D. Guo, Y. Guo, Y. Huang, Y. Chen, X. Dong, H. Chen, and S. Li, *Chemosphere*, **265**, 129126 (2021).
- M. A. Ganzoury, S. Ghasemian, N. Zhang, M. Yagar, and C.-F. de Lannoy, *Chemosphere*, **286**, 131600 (2021).
- M. F. Ahmadi, A. R. L. da Silva, C. A. Martínez-Huitile, and N. Bensalah, *Electrochim. Acta*, **369**, 137688 (2021).
- L. Candido and J. A. C. P. Gomes, *Mater. Chem. Phys.*, **129**, 1146 (2011).
- P. Mandal, M. K. Yadav, A. K. Gupta, and B. K. Dubey, *Sep. Purif. Technol.*, **247**, 116910 (2020).
- Y. J. Shih, S. H. Huang, C. L. Chen, C. D. Dong, and C. P. Huang, *Electrochim. Acta*, **360**, 136990 (2020).
- Y. Yang and M. R. Hoffmann, *Environ. Sci. Technol.*, **50**, 11888 (2016).
- C. Zhang, D. He, J. Ma, and T. D. Waite, *Water Res.*, **145**, 220 (2018).
- X. Meng et al., *Sep. Purif. Technol.*, **235**, 116233 (2020).
- Y. Yang, J. Shin, J. T. Jasper, and M. R. Hoffmann, *Environ. Sci. Technol.*, **50**, 8780 (2016).